Finite Element Analysis of Tubing Buckling in Oil Wells

Jueren Xie

C-FER Technologies Inc. Canada

***Abstract**: In oil wells, there are numerous reported field cases of tubing buckling during the installation and operation. The tubing buckling mode typically starts with a single lateral wave, which with increased compression transitions into multiple waves and then into a helically buckled configuration within the borehole or cased hole. Traditionally, analytical equations have been used to predict tubular string buckling in wells. However, such analytical solutions have been found to be suitable only for idealized conditions, such as elastic material and uniform geometric conditions. In this paper, Abaqus Finite Element Analysis (FEA), with consideration of material plasticity and pipe-in-pipe contact, was used to perform the buckling analysis of tubular strings. This paper proposes an FEA-based design approach, which takes into account of the post-buckling behavior of the tubing string, to achieve the improved certainty, integrity, safety and economy of the design. Two case studies are presented to demonstrate the use of the proposed approach. Through analysis examples, this paper presents discussions on the impact of friction force and nonconservative forces, such as tubing end pressure loading.*

***Keywords**: Analysis, Buckling, Buoyancy Force, Casing, Collapse, Curvature, Deformation, Design, Failure, Flexural Strain, Formation, Friction, Gap, Helical Buckling, Nonconservative Force, Oil Well, Plasticity, Stiffness, Strain, Stress, Tubing, Yield Strength*

1. Introduction

Buckling is a mathematical instability that can lead to a failure mode. In oil wells, there are numerous reported field cases of tubing strings buckled under axial compressive loading. During the well installation, the compressive forces may arise from friction between the tubing and the drilled borehole or casing wall, or due to the blockages such as debris and mechanical barriers. As the tubing is exposed to wellbore drilling mud or completion fluids during installation, the tubing is subjected to buoyancy forces. Not that the buoyancy forces have been considered by many as a contributor to tubing buckling in vertical wells, although their impact on tubing warrants a further discussion as presented in this paper. During operation, temperature and pressure changes may also cause casing and tubing strings to buckle when they are constrained by the formation, mechanical anchors or potential barriers or other blockages (Xie et al 2016).

Tubing buckling modes can typically be characterized first by a single lateral wave, followed by multiple waves (which some have referred to as sinusoidal buckling) and ultimately by helically buckled configurations as compressive loading is increased. Figure 1 presents a schematic representation of multiple tubing strings buckled inside a section of wellbore casing or a liner.

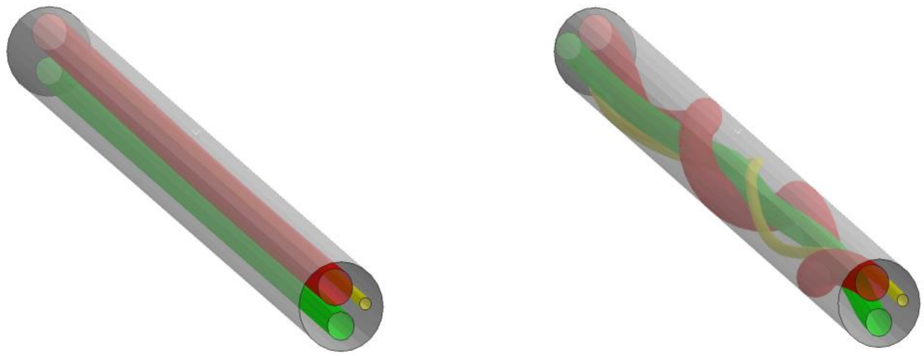

(a) Before buckling **(b) After buckling**

Figure 1. Schematic representation of multiple string tubing buckling.

Traditionally, analytical equations have been used to predict tubular string buckling in wells, and as a design basis to prevent the occurrence and impacts of buckling. However, such analytical solutions have been found to be suitable only for idealized conditions, such as elastic material and uniform geometric scenarios. Furthermore, the design basis to prevent buckling appears to be overly conservative and unrealistic. First, the long unsupported length of a tubing string often presents a very small critical loading for lateral and helical buckling, which is typically lower than the load requirement for installation. Second, a buckled tubing string can sustain further axial compressive loading by reducing the helical pitch, generally provided that the tubing string remains elastic.

In contrast to the traditional design approach that attempts to avoid the occurrence of moderate elastic buckling, an advanced design approach should employ a criterion to prevent the occurrence of material plasticity. This would require, however, the calculation of both the axial strain related to axial loading, and the flexural strain resulting from buckling. To consider the post-buckling behavior of the tubing string and the impact of flexural strain, Finite Element Analyses (FEA) is required to model the non-linear behavior related to the contact interaction between tubing and casing, and the material plasticity.

This paper presents a methodology of using FEA to assist in tubular design for wells where buckling may occur. Abaqus FEA, with consideration of material plasticity and pipe-in-pipe contact, was used to determine the tubing deformation resulting from buckling. Two case studies are presented to demonstrate the proposed approach to achieve improved certainty, integrity, safety and economy of the tubular designs for oil and gas wells. Through these two analysis examples, this paper illustrates the impact of friction force and nonconservative forces such as tubing end pressure loading.

2. Tubing Load Design Considerations

2.1 Installation Load Requirement

To successfully install a tubing string to the target depth in a well, it is necessary that the applied force be greater than the total resistive force, i.e.

$$F_{Applied} \geq F_{Resistive} \qquad \text{[Equation 1]}$$

The applied force, $F_{Applied}$, can include the self weight of tubing strings, and any applied loading at wellhead.

The resistive force, $F_{Resistive}$, can develop in the tubing string and may include the following forces:

- Friction force between the tubing and the casing/liner or borehole wall;
- Drag, friction and blockage due to debris such as scale on the casing surface or sand accumulated in inclined and horizontal sections of the wellbore;
- Mechanical barriers (e.g. tubing collars and crossovers, liner hangers, downhole monitoring devices, steam distribution devices, artificial lift equipment); and
- Interference and entanglement with other tubing strings in the well (e.g., as illustrated in Figure 1(b)).

In vertical wells, buoyancy forces acting on the lower end of a tubing string have also been considered by many as one of the loading mechanisms responsible for tubing buckling. However, the hydrostatic pressure force, which acts normal to the tubing surface and is often also then tangential to the tubing axis, may also be considered as a nonconservative force, by which the static criterion may not be adequate to predict buckling (Timoshenko et al 1961). An analysis example is included in this paper to examine the potential for tubing buckling due to buoyancy forces.

Intuitively, and as described by Equation 1, as the resistive force increases during installation, a higher applied force will be required to continue to run a tubing string into a well. If this applied compressive force becomes sufficient, significant tubing buckling may develop, and eventually localized yielding and significant permanent deformation may occur. Therefore, to avoid possible mechanical failure of the tubing strings, the applied force should always be controlled such that it is less than the tubing string design load limit, F_{Limit}, i.e.

$$F_{Applied} \leq F_{Limit} \qquad \text{[Equation 2]}$$

Combining Eqns. (1) and (2), it is apparent that the following relationship must apply:

$$F_{Resistive} \leq F_{Limit} \qquad \text{[Equation 3]}$$

That is, in order to successfully install a tubing string (e.g. without permanently damaging or failing the string), the maximum resistive force should not exceed the tubing design load limit.

2.2 Tubing Load Limit

Under uniaxial compressive loading, the tubing load carrying capacity can be defined as the maximum axial compressive loading that a tubing string can sustain. Similarly, the tubing load design limit can be defined as the allowable load carrying capacity to some selected maximum used in the design (e.g., a percentage of the yield load).

2.2.1 Load Limit Based on Analytical Solutions

Traditional tubing string designs have made use of analytical equations aimed to prevent the occurrence of elastic buckling of tubing strings. As a result, the load limits were typically presented in terms of tubing cross-sectional properties (OD and thickness) and elastic modulus (i.e. Young's modulus).

Lubinski (1950) and Wu (1992) studied tubing buckling in vertical wells. Wu (1992) suggested that, under axial compressive loading, the tubing can buckle in the vertical section first in the sinusoidal mode, followed by buckling in a helical configuration. Wu presented the following equations for the critical axial compressive load to initiate the sinusoidal buckling (F_{cr}) and helical buckling (F_{hel}) modes in a vertical wellbore:

$$F_{cr} = 2.55(EIW_e^2)^{1/3} \qquad \text{(Sinusoidal buckling in vertical section)} \qquad \text{[Equation 4]}$$

$$F_{hel} = 5.5(EIW_e^2)^{1/3} \qquad \text{(Helical buckling in vertical section)} \qquad \text{[Equation 5]}$$

where E is the Young's modulus of the tubing material, I is the moment of inertia of the cross section of the tubing, and W_e is the effective tubing weight in the wellbore fluid.

Others, including Dawson and Paslay (1985), Wu (1992), Kuru, Martinez and Miska (1999), and Miska and Cunha (1995) studied tubing buckling issues in directional and horizontal wells, while Chen et al. (1989, 1990), Wu (1992), and Wu and Juvkam-Wold (1993a, 1993b) studied tubing buckling in horizontal wells.

Lubinski et al (1961) presented the following equation to relate the pitch of helically buckled tubing (p) to the axial compressive force (F).

$$p = \pi\sqrt{\frac{8EI}{F}} \qquad \text{[Equation 6]}$$

2.2.2 Load Limit Based on FEA Solutions

Using an FEA-based design approach, the load limit of a string can be determined as the load corresponding to the onset of plastic deformation. In order to accurately capture this load limit, the FEA should be able to simulate the initiation of lateral and helical buckling, impacts on local curvature as a function of helical pitch, and the material plasticity behaviour. Therefore, the tubing load limit determined by FEA will be an implicit function of tubing cross-sectional properties (OD and thickness), the clearance between tubing OD and casing/liner or borehole ID (see Figure 2a), and tubular material properties (Young's modulus, Poisson's ratio, and yield strength).

In this paper, Abaqus FEA, with consideration of material plasticity and pipe-in-pipe contact, was used to determine the tubing deformation resulting from buckling. As shown in Figure 2(b), the tubing string was modeled using three-dimensional beam elements which are capable of tracking large out-of-plane deformations. A discrete annular gap was prescribed between the tubing OD and the casing ID. The interaction between the buckled tubing and the casing or borehole wall was modeled using pipe-in-pipe contact elements ITT3 (Abaqus 2018). In this paper, an outer casing boundary was assumed and was modeled as a rigid surface. In order to simulate the buckling, non-linear geometric analysis (NLGEOM) was performed, and a small geometric imperfection was assumed in the tubing. Note that by using NLGEOM, the pressure loading on the tubing was modeled as the follower forces.

The tubing material was modeled using the elastic-plastic constitutive relationship.

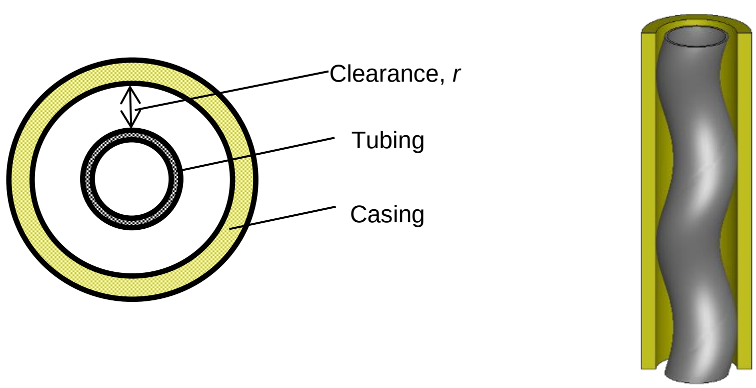

(a) Tubing clearance **(b) FEA model for buckling**

Figure 2 Schematic representation of (a) tubing clearance and (b) FEA model for buckling.

3. Case Study 1 – Determination of Tubing Load Limit

3.1 Case Description

This first case study demonstrates determination of the load limit for an 88.9 mm OD, 15.2 kg/m weight C110 material grade (API 5CT 2012) tubing string subjected to axial compressive force. The model considered 100 m length of vertical tubing string, with a concentrated axial load applied to one end of the string (the moving end), and fixed boundary condition at the other end (see Figure 3A). The interaction between tubing OD and casing ID was modeled using pipe-in-pipe contact elements, with the friction coefficient assumed to be 0.35, which is slightly greater than 0.3 assumed by Wu, et. al. (1995). The clearance between tubing ID and casing OD was assumed to be 13.3 mm, which is the radial difference between the tubing OD and the ID of 139 mm, 38.7 kg/m casing. Mesh density of 50 mm per beam element was used in the model.

3.2 Analysis Results

Figure 3 presents the contour plots of lateral displacement of the tubing at a number of load points, labeled as A to G corresponding to increasing elastic (A to D) and plastic (E to G) load and strain values shown. These load points are highlighted in the curvature and plastic strain vs. axial force curves presented in Figure 4.

As shown in Figures 3 and 4, the deformed shape of the tubing changes significantly with the axial loading. At load point A (66.9 kN), a lateral buckling mode is evident. As the load increases to load point B (158 kN), a helical buckling mode is observed (see the end view plot). As the load increases from load points B to E, the pitch of helical buckling decreases with an increasing number of helices being developed over the model length. At approximately load point E, plastic strain is observed in the tubing section near the load end. From load points E to G, significant curvature and plastic strain values develop in the critical section resulting in structural damage of the tubing.

Figure 5 presents the FEA results of the relationship between the helical buckling pitch and the axial compressive force, both of which were the values recorded near the moving end of the tubing. The pitch predicted using Equation 2 (Lubinski 1961) is also shown for the elastic range. As can be seen, the helical buckling pitch decreases as the axial force was increased. Figure 5 shows that the FEA results show reasonably good agreement with the results predicted using Equation 2.

Using Equations 4 and 5, the critical load for lateral buckling was estimated at 4.87 kN, and for the onset of helical bucking was 10.6 kN. These critical loads are significantly lower than the 1087 kN value corresponding to the predicted elastic load limit obtained from this FEA study. This analysis example demonstrates that the critical loads predicted using these analytical equations appear to provide values that for design purposes are overly conservative.

Step	A	B	C	D	E	F	G
Load (kN)	66.9	158	344	685	1087	1294	1719
Plastic Strain	0%	0%	0%	0%	0.02%	0.43%	11.9%
Side View of Lateral Displacement over 100 m Model Length 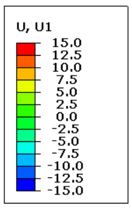 Unit: mm	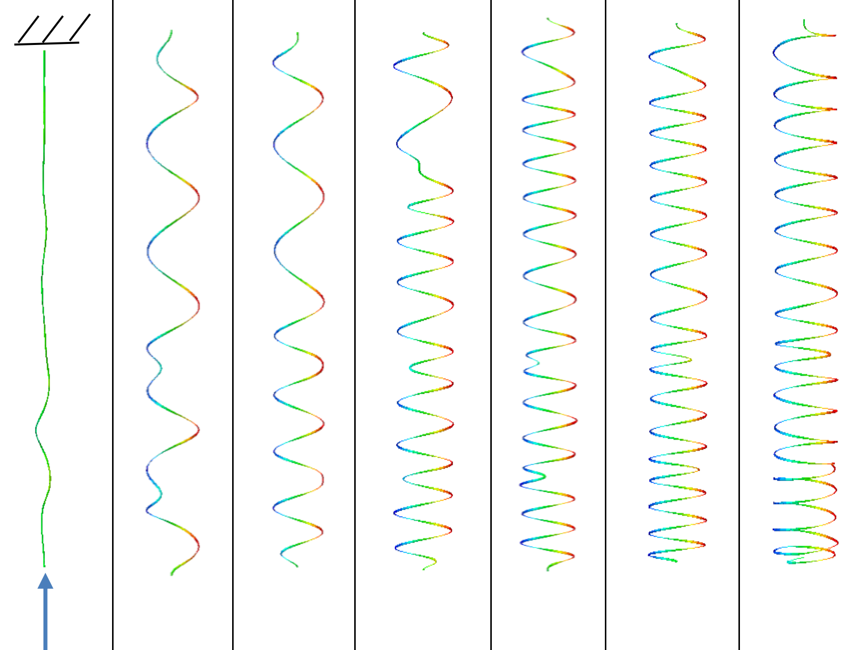						
End View							

Figure 3. Contour plots of lateral displacement over the development of helical buckling for 88.9 mm, 15.2 kg/m C110 tubing. (Lateral displacement was magnified)

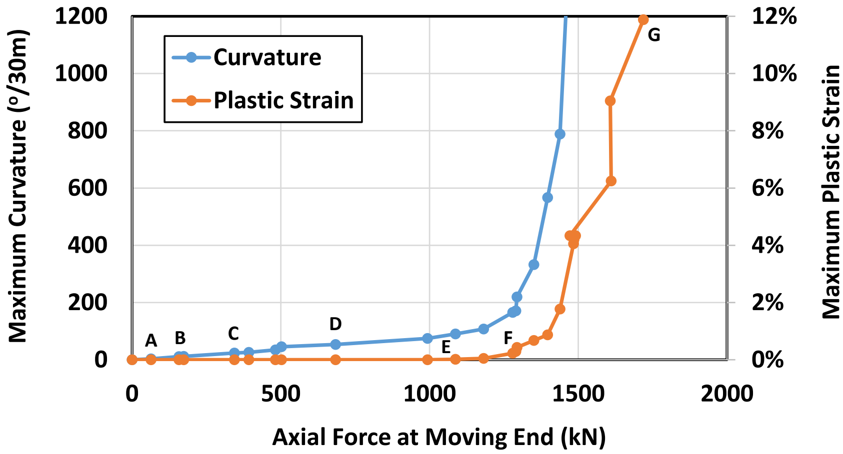

Figure 4. Curvature and plastic strain vs. axial force for 88.9 mm, 15.2 kg/m C110 tubing.

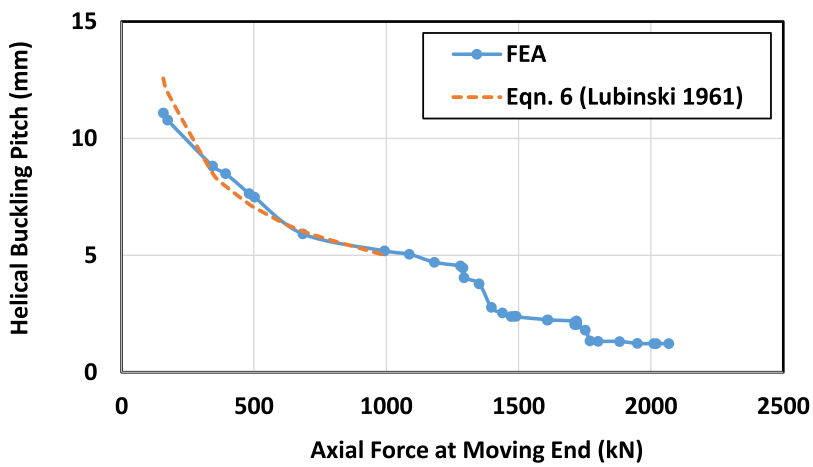

Figure 5. Helical buckling pitch vs. axial force for 88.9 mm, 15.2 kg/m C110 tubing.

3.3 Effect of Friction Force

Figure 6 presents the results of the friction force over the 100 m model length, based on the parametric analyses to study the impact of friction coefficient on the ability to transmit force in the well. As can be seen, there is no friction with zero friction coefficient, and the axial force at the fixed end should remain the same at the moving end (i.e., the tubing is moving). As the friction coefficient increases, the friction force increases at the same level of axial force at the moving end. For the case with the friction coefficient of 0.35, which was studied in Figures 3 to 5, at the elastic limit of 1087 kN, the friction force is approximately 25% of the axial force at the moving end.

As one would expect, as the friction force and/or length increase, the ability to transmit force along the tubing string to overcome friction and continue to move the tubing string down the well are reduced. When the friction force between the tubing and casing becomes sufficiently large, "lock-up" occurs where the tubing string can no longer be moved in the well. That is, build-up of the friction force reaches the magnitude required to further advance the tubing string in the well.

To study the impact of friction force on "lock-up", parametric analyses were performed for the 0.35 friction coefficient case with tubing model lengths of 100, 200, 500 and 1000 m. Figure 7 presents the contour plots of axial force corresponding to the elastic limit (i.e. 1087 kN). For all of these cases, the axial force decrease over the length due to the friction effect. At the elastic limit, the friction forces over the model length are 25%, 40%, 61% and 76%, respectively, as compared to the force at the moving end. It suggests that the "lock-up" potential increases with the buckled length. It is also noted that due to the variation in the axial force, the pitch of helical buckling increase over the length, with the smallest pitch at the moving end and the largest at the fixed end, suggesting that the tubing near the moving end is more critical for failure due to buckling.

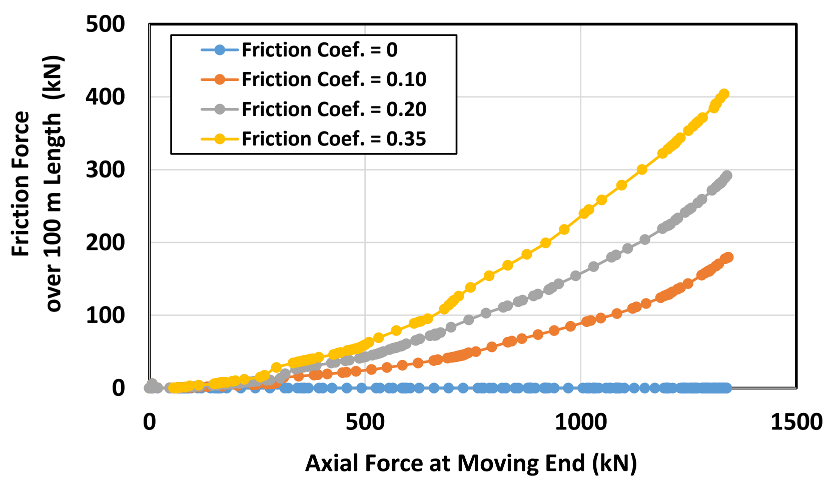

Figure 6. Friction force vs. axial force at moving end for 88.9 mm, 15.2 kg/m C110 tubing with 100 m model length.

Model Length	100 m	200 m	500 m	1000 m
Friction Force vs. Moving End Force	25%	40%	61%	76%
Axial Force (N) Over Model Length 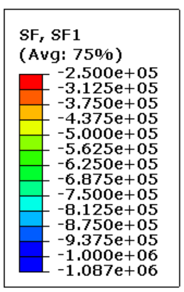 			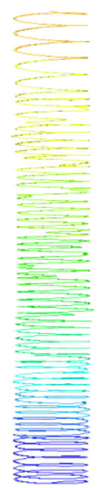	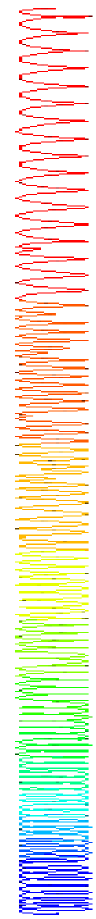

Figure 7. Contour plots of axial force at elastic limit for 88.9 mm, 15.2 kg/m C110 tubing with various model lengths and 0.35 friction coefficient. (Lateral displacement was magnified)

4. Case Study 2 – Impact of Buoyancy Force in Deep Wells

4.1 Case Description

The second case study demonstrates the impact of buoyancy force on tubing loading and response in deep vertical wells. The well is 6600 m deep with the tubing string consists of Tubing 1 (88.9 mm OD×76 mm ID C110 down to 6100 m); and Tubing 2 (93.2 mm OD×73.2 mm ID C110 from 6100 to 6600 m). The interaction between the tubing string OD and the casing ID was modeled using pipe-in-pipe contact elements, with a friction coefficient of 0.35. The radial clearance between the tubing OD and casing ID was 13.3 mm for Tubing 1, and 11.2 mm for Tubing 2. Mesh density of 200 mm per beam element was used in the model.

During installation, the tubing string was inserted into a full vertical column of drilling mud which has a density of 1920 kg/m^3. As a result, a buoyancy force will be generated on the bottom-end of the tubing string. To examine the difference in the tubing response to the buoyancy force versus an applied force, the bottom-end force was modeled using two different approaches: (1) as a pressure loading distributed over the tubing end face; and (2) as a vertical upward force located at the centre axis of the end face.

4.2 Analysis Results

<u>Solution 1 – Bottom-end Force Modeled As Pressure Loading</u>

The installation of the tubing string was modeled in two steps. First, gravity loading was applied to the entire tubing string for the calculation of the hanging weight. Second, the drilling mud was modeled as a pressure gradient loading on the tubing ID, OD and the bottom-end section corresponding to the hydrostatic pressure of the mud column. When the non-linear geometry analysis (NLGEOM) was performed for the buckling problem, the pressure loading is considered as the follower force.

Figure 8(a) presents the analysis results of the axial force distribution of the tubing string (on the left side of the figure). At the surface, the tubing is subjected to 644 kN of tensile force corresponding to the hanging weight of the tubing string in the column of drilling mud. At the bottom end, the tubing is subjected to 328 kN of compressive force, due to the mud pressure loading. As a result, the tubing string is subjected to 385 MPa tensile stress at the surface, and 126 MPa compressive stress at the bottom-end. These two stress values are lower than the 758 MPa yield strength of the C110 grade of tubular material (API 5Ct 2012).

Figure 8(b) presents the contour plot of tubing curvature. Examination of the analysis results for this solution shows that no buckling developed and that the maximum curvature located near the bottom-end of the tubing string was found to be 0.002°/30m.

Solution 2 – Bottom-end Force Modeled Vertically

As a comparison to the pressure loading, an equivalent bottom-end loading (resulting from the column of drilling mud) was modeled as a vertical concentrated force. The contour plot of the tubing curvature is presented in Figure 8c. The results for this case show that over the lower portion of the well, the tubing string experienced helical buckling with a maximum curvature of 11.2°/30m.

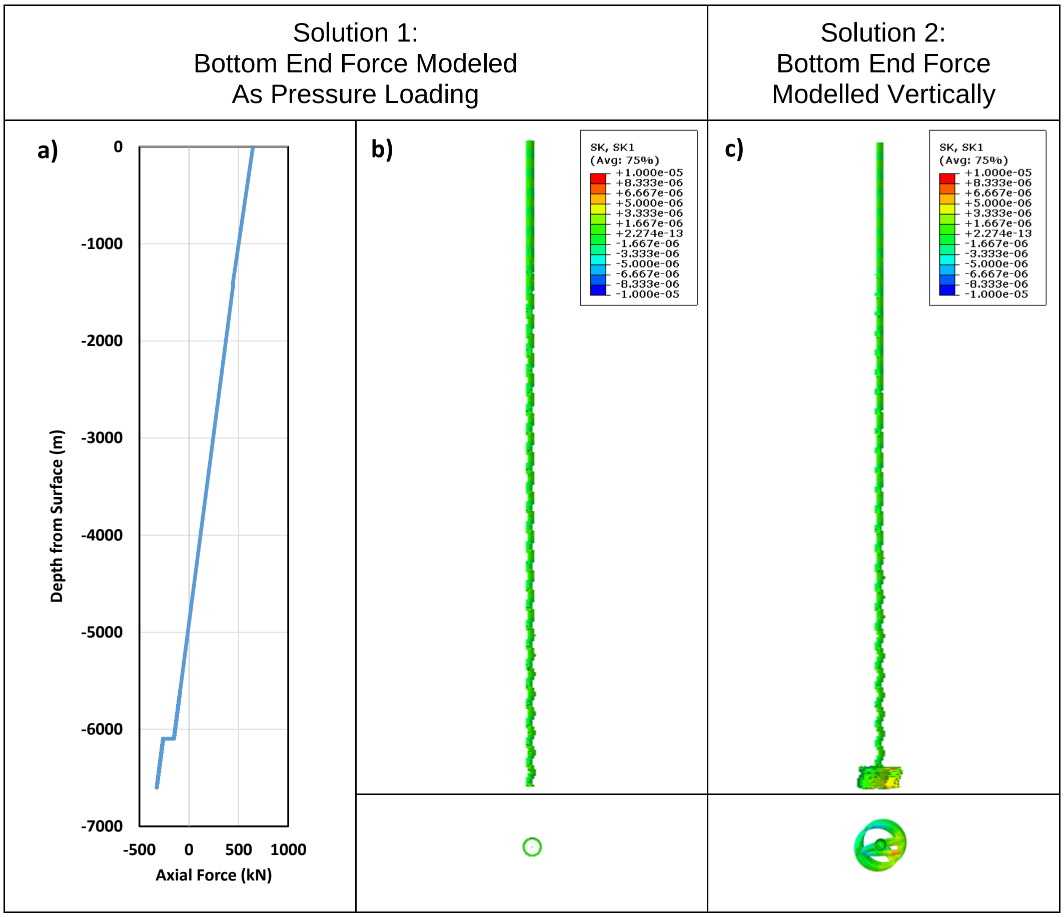

Figure 8. Contour plots of curvature as predicted by two different modeling approaches (Lateral displacement was magnified)

4.3 Discussion on Conservative vs. Nonconservative Forces

The significantly different results obtained for the two solution approaches presented above warrants a discussion on the nature of the pressure loading from a column of fluid versus the application of a concentrated force load.

In the second approach (solution 2), the work done during a displacement depends only on the initial and final positions and is independent of the path of the point of application of the force. Such loading scenarios are considered to be conservative loads, and the resulting buckling can be analyzed using static methods, as described by to Timoshenko et al (1961).

In the first modeling approach (solution 1), however, during the non-linear geometry analysis, because the force is a normal pressure force (i.e. as follower), the bottom-end pressure force would remain acting in the direction tangent to the deflection curve. Such loading scenarios are considered to be nonconservative loading, as it is not possible to calculate the work done by the force during buckling on the basis of the initial position.

As mentioned by Timoshenko et al (1961), in the case of nonconservative forces, the static method may prove inadequate, and instead, a dynamic criterion of stability should be used for the buckling analysis. Timoshenko et al noted that a progressive growing of amplitude of vibrations can be considered as the dynamic instability or perturbation for analyzing such load scenarios. Timoshenko et al presented an example of a cantilever subjected to a concentrated compressive force acting tangentially to the beam axis. The natural frequency was expressed in terms of the compressive force and it was shown that, as the compressive force was increased, the first frequency would approach to the second frequency. When the first and second frequencies coincide, the system becomes dynamically unstable.

Using the similar approach by Timoshenko et al, dynamic analysis was performed on the tubing system of this case study following the solution 1 (i.e. the bottom end force modeled as a pressure loading). In addition to the tubing weight, add-masses related to the enclosed and attached fluid were assigned to the beam nodes. The analysis shows that the first two frequencies are 4.31×10^{-3} and 9.66×10^{-3} cycle/second, respectively for the case studied with mud density of 1920 kg/m^3. Figure 9 presents the frequency vs. mud density based on the parametric analysis. Note that the end compressive force increases with the mud density. The analysis shows that as the mud density increases from 1000 to 2400 kg/m^3, both the first and second order frequencies decrease. Although these frequency trends are approaching one another, they remain separated for a very wide range of mud density values examined. This dynamic stability analysis suggests that the dynamic buckling is unlikely to occur for this case.

Furthermore, these results suggest that the mud pressure alone does not present a potential to cause tubing buckling in the case analyzed. However, it is possible that a conservative loading mechanism is introduced by any changes in the force and boundary conditions to the system. Therefore, the tubing buckling deformation remains a critical consideration for the deep vertical well applications.

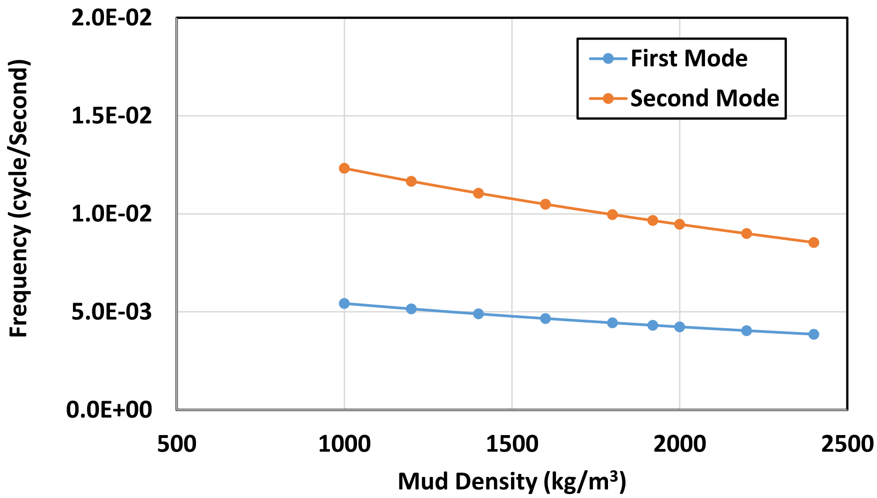

Figure 9. Frequency vs. mud density.

5. Summary

This paper presents the results of an Abaqus FEA study examining tubing buckling behaviour in oil wells, with consideration of factors not commonly included in analytical solutions, such as material plasticity and pipe-in-pipe contact. Two case studies were presented to demonstrate the proposed approach to achieve the safety and economy of the tubing string design for oil wells. In addition, through the analysis examples, this paper presents discussions on the impact of friction force, and the impact of the nonconservative force developed at the tubing end by the column of fluid generating pressure end loading which is tangential to tubing axis.

6. Acknowledgement

Support and funding for the preparation of this paper was provided by C-FER Technologies (1999) Inc. Technical review of the paper was performed by Todd Zahacy, Senior Engineering Consultant – Exploration and Production at C-FER Technologies, and his assistance is sincerely appreciated. In addition, the author would like to acknowledge the contributions from Yi Fang and Chengye Fan, who performed literature reviews and modeling in past studies in the area of wellbore tubular buckling while Research Engineers at C-FER Technologies.

7. References

1. Abaqus User's Manual, Version 6.18, Dassault Systémes Simulia Corp., Providence, RI.
2. American Petroleum Institute (API) 2012. API Specification 5CT: Specification for Casing and Tubing. Ninth Edition. January 1.
3. Chen, Y.C., Lin, Y.H. and Cheatham, J.B. 1989. "An Analysis of Tubing and Casing Buckling in Horizontal Wells". Paper presented at the 21st Annual OTC, Houston, TX, USA.
4. Chen, Y.C., Lin, Y.H. and Cheatham, J.B. 1990. "Tubing and Casing Buckling in Horizontal Wells". JPT, February, pp. 140-141.
5. Cunha, J.C.S. 1995. Buckling Behavior of Tubing in Oil and Gas Wells. A Theoretical and Experimental Study with Emphasis on the Torque Effect. PhD dissertation, The University of Tulsa.
6. Dawson, R. and Paslay, P.R. 1985. "Drillpipe Buckling in Inclined Holes". JPT, October, pp. 1734-1738.
7. Kuru, E., Martinez, A. and Miska S. 1999. "The Buckling Behavior of Pipes and Its Influence on the Axial Force Transfer in Directional Wells". Paper SPE/IADC 52840 presented at 1999 SPE/IADC Drilling Conference, Amsterdam, Holland, March 9-11.
8. Lubinski, A. 1950. "A Study on the Buckling of Rotary Strings". API Drilling Production Practice, pp. 178-214.
9. Lubinski, A. et al, "Helical Buckling of Tubing Seal in Packers", Petroleum Transactions, 86th Annual Fall Meeting of SPE, Oct. 8-11, 2961, Dallas, USA.
10. Miska, S., and Cunha, J.C.S. 1995. "An Analysis of Helical Buckling of Tubular Subjected to Axial and Torsional Loading in Inclined Wellbores". Paper No. SPE 29460 presented at the Operations Symposium, Oklahoma City, OK, April.
11. Timoshenko, S. P. and Gere, J. M., Theory of Elastic Stability, Second Edition, Dover Publications, INC., 1961.
12. Wu, J., 1992. "Buckling Behaviour of Pipes in Directional and Horizontal Wells". PhD dissertation, Texas A&M University.
13. Wu, J. and Juvkam-Wold, H.C. 1993a. "Study of Helical Buckling of Pipes in Horizontal Wells". SPE Production Operations Symposium, Okahoma City, OK, US, March 21-23.
14. Wu, J. and Juvkam-Wold, H.C. 1993b. "Helical Buckling of Pipes in Extended Reach and Horizontal Wells – Part 2: Frictional Drag Analysis". Journal of Energy Resources Technology, September.
15. Wu, J. and Juvkam-Wold, H.C. 1995. "Coiled Tubing Buckling Implication in Drilling and Completing Horizontal Wells". SPE Drilling and Completions, March.
16. Xie, J., Matthews, C. M. and Dessein, T. "Finite Element Analysis for Understanding Oil and Gas Well Deformation Mechanisms", Science in the Age of Experience, 2016.